Frontiers in Heat and Mass Transfer (FHMT), 16, 20 (2021)
DOI: 10.5098/hmt.16.20

Global Digital Central
ISSN: 2151-8629

Frontiers in Heat and Mass Transfer

Available at www.ThermalFluidsCentral.org

NUMERICAL INVESTIGATION OF NUSSELT NUMBER FOR NANOFLUIDS FLOW IN AN INCLINED CYLINDER

Kafel Azeez Mohammed[a,**], Ahmed Mustaffa Saleem[b], Zain alabdeen H. Obaid[a]

[a] *Research Center of Renewable Energy, University of Anbar /Iraq*
[b] *Department of Power Mechanics Technology, Engineering Technical College/Mosul, Northern Technical University/Iraq*

ABSTRACT

Numerical investigation is performed for the determination of Nusselt number of ZnO, TiO_2 and SiO_2 nanoparticles dispersed in 60% ethylene glycol and 40% water inside inclined cylinder for adiabatic and isothermal process. The present study was conducted for both the constant heat flux (10,000 W/m^2) and constant wall temperature (313.15 K) boundary conditions. At the inlet, the uniform axial velocity and initial temperature (293 K) were assumed. The results show the change of average Nusselt number at Reynolds number (400), Rayleigh number (10^6) and volume fraction percentage (2%). From results for adiabatic process when increasing the slop up to (45°), the Nusselt number augments, while Nusselt number is reduced by further tube inclination. As it is clearly seen, the highest value of Nusselt number is corresponded to (45°) and for isothermal process it is shown that the value of Nusselt number in horizontal position is higher than the vertical position. The values of Nusselt number ratio were evaluated to be (45%, 31%, 25%) for the three Nano fluids (ZnO, TiO2 and SiO_2) respectively, with the insulation (adiabatic) and (36%, 27%, 22%) without insulation (isothermal).

Keywords: *concentration nanofluids, ethylene glycol, nanofluids, nanoparticles, thermal conductivity*

1. INTRODUCTION

Nanofluids are suspensions of nanometer-size particles, generally smaller than 100 nm average particle size, suspended in base fluids such as water, ethylene glycol, propylene glycol and oil. With increasing energy demand of the modern society, nanofluid research has received great attention due to the thermal energy efficiency, resulting from the enhanced thermal characteristics of nanofluids with heat exchangers, heat sinks and solar collectors (Farhan et al., 2020) etc.

Nguyen and Menn (2009) had numerically studied the problem of a forced laminar flow and heat transfer of Al2O3-water nanofluid, with two different particle sizes, 36nm and 47 nm, inside a two-dimensional flat microchannel. Both the single-phase fluid and two-phase fluid models were used. Some significant results showing the effects due to the use of nanofluid on the heat transfer coefficient as well as the comparison of between the two models are presented and discussed. Shariat et al. (2011) laminar mixed convection Al2O3-water nanofluid flow in elliptic pipes with different aspect ratio (AR) had been investigated, employing the Brownian motions of nanoparticles for determining the thermal conductivity and dynamics viscosity of Al2O3-Water nanofluid, which depend on temperature. The axial velocity, secondary flow pattern, contours of temperature, distribution of nanoparticles, skin friction factor and Nusselt number profiles were presented and discussed. Sahoo et al. (2012) had focused on determining the thermal conductivity of 60:40 EG/W based SiO2 nanofluid. The 60:40 mass ratio is chosen because it guarantees no freezing, and subsequently no damage to the equipment, down to -48.3 oC as per the ASHRAE data. The particle volumetric concentrations up to 10% had been experimentally investigated. This concentration may be too high requiring a large pumping power in applications as heat transfer fluid. However, it gives us a broader database and establishes a general trend of the variation of thermal conductivity with concentration.

Ahmed et al. (2014) investigated the boundary layer flow and heat transfer characteristics due to stretching tube when the tube surface was permeable in the presence of heat source/sink utilizing nanofluids. The effects due to uncertainties of thermal conductivity and dynamic viscosity had been also investigated. Abdellateef (2016) investigated the peristaltic transport of Nano viscous incompressible Newtonian fluid in an inclined annulus tube under the assumptions of long wavelength and lower Reynolds number. Attention has been focused on the behaviors of Brownian motion parameter (Nb), thermophoresis parameter (Nt) and inclination of the annulus cylinder. The result indicated an appreciable increase in the temperature and Nanoparticles concentration with the increase in the strength of Brownian motion effects, and the inclination angle increases the pressure and all these also discussed through graphs. Hekmatipour et al. (2017) the mixed convective heat transfer and pressure drop characteristics of a buoyancy-aided nanofluid flow in a vertical tube was investigated experimentally. As such, this research was conducted to study the effect of using copper oxide nanoparticles on the heat transfer and pressure drop characteristics of the heat transfer oil flow. The tube wall temperature was constant and the flow rate was low enough to ensure that the flow regime was always laminar.

Davarnejad and Hekmat (2018) a new correlation for the dynamic viscosity prediction was applied. The simulation was carried out in a fully developed turbulent regime. The conditions were exactly extracted from the experimental work of Heris (2006). The simulated data (obtained from two models: mixture and VOF model) were compared with each other and the experimental ones. Kandwal et al. (2019) investigations were concentrated on exploring the performance of nanofluid flow through different geometries. They utilized several latest methods to describe the prevailing equations with various conditions, but they

* Corresponding author. Email: kafelazeez1966@uoanbar.edu.iq

Global Digital Central
ISSN: 2151-8629

ignored the combined action of heat generation (or absorption) and viscous dissipation on inclined cylinder due to suction/injection and solid volume fraction of nanoparticles. Raei and Peyghambarzadeh (2019) an experimental studied had been performed to measure local convective heat transfer coefficient and friction factor of stabilized γ-Al2O3/water nanofluid in a fully-developed turbulent flow regime in a double tube heat exchanger. Experiments performed at different nanofluid concentrations, operating temperatures, and nanofluid flow rates. Jalali et al. (2020) used nanofluids and downward flow to improve the convective heat transfer under constant wall temperature. There were a couple of numerical articles which were qualified to predict the experimental result. Sometimes, the numerical outcomes were against experimental results Hekmatipour et al. (2019), Hekmatipour and Jalali (2020). Therefore, numerical model was not displayed in this research. Therefore, the introduction of correlation in downward flow was valuable. The impact of using copper oxide-thermal oil nanofluid and inclination angle on the convective heat transfer and pressure drop in the slope circular tube was analyzed empirically. The boundary condition was really important in experimental analysis. Qiu et al. (2020) provided a comprehensive state-of-the-art review of the thermo physical properties of nanoscale materials. The review was presented in two parts, the first part (Part I) mainly introduced the latest research progress on thermo physical properties of solid nanostructured materials, which included theoretical and experimental research advances in k, cp, and thermal diffusivity (α). The second part (Part II), mainly introduced the latest research progress on the thermo physical properties of nanofluids, including various mathematical models (from classical to advanced models), experimental measurement techniques, theory vs. experiments and the main factors affecting the k, cp, ρ, μ and heat transfer rate of nanofluids. In addition, studied on molecular dynamic (MD) simulation that was used for modeling the properties at the nanoscale were reviewed.

In the present study, numerical investigation was carried out for the determination of Nusselt number of ZnO, TiO2 and SiO2 nanoparticles dispersed in 60% ethylene glycol and 40% water inside inclined cylinder for adiabatic and isothermal process.

2. GOVERNING EQUATION AND FORMULATION

Fig. 1 shows a schematic diagram of tube (D=0.015 m and Z=2 m) with uniform heat flux. The fluid in the tube is a water-based nanofluid containing different types of nanoparticles such as (TiO_2, ZnO and SiO_2). It is assumed that the base fluid (60% ethylene glycol and 40%water) and nanoparticles are in thermal equilibrium and no slip accurse between them. The thermo–physical properties of the nanofluid are assumed to be constant. The governing equations for the laminar, steady and single phase fluid (Homogenous model).

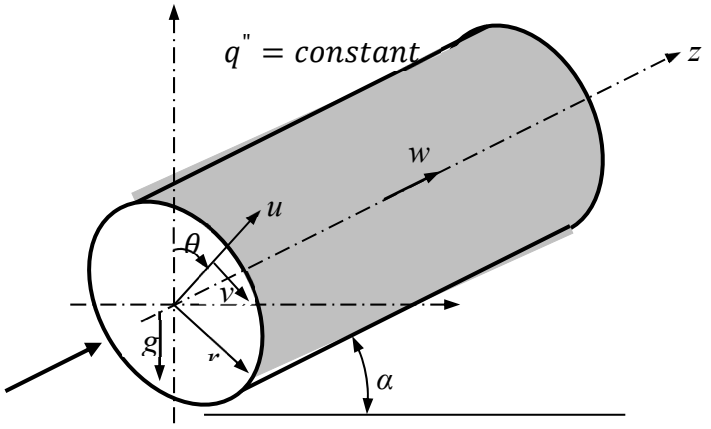

Fig. 1 Physical representation of the considered

Continuity Equation

The equation of conservation of mass in the cylindrical coordinates is given as, (Shareef et al., 2010).

$$\rho_{nf}\frac{\partial(ru)}{\partial r}+\frac{\rho_{nf}}{r}\frac{\partial v}{\partial\theta}+\rho_{nf}\frac{\partial w}{\partial z}=0 \quad (1)$$

where:
ρ_{nf} - Density of the nanofluid, (kg/m3)
r - Inner radius of cylinder, (m)
u - Radial velocity component (r), (m/s)
v - Tangential velocity component (θ), (m/s)
w - Axial velocity component (z), (m/s)
θ - Tangential coordinate (Degree).
And, by using the second assumption (i.e., w = 0), equation (1) can be reduced to the following form:

$$\rho_{nf}\frac{\partial(ru)}{\partial r}+\frac{\rho_{nf}}{r}\frac{\partial v}{\partial\theta}=0 \quad (2)$$

Momentum Equations

The equations of conservation of momentum in the cylindrical coordinates in the radial, tangential, and axial directions (r, θ, z, respectively) can be written, (Shareef et al., 2010).

r -component

$$\rho_{nf}\left(u\frac{\partial u}{\partial r}+\frac{v}{r}\frac{\partial u}{\partial\theta}-\frac{v^2}{r}\right)=-P_r+\mu_{nf}\left(\frac{\partial^2u}{\partial r^2}+\frac{1}{r}\frac{\partial u}{\partial r}+\frac{1}{r^2}\frac{\partial^2u}{\partial\theta^2}-\frac{u}{r^2}-\frac{2}{r^2}\frac{\partial v}{\partial\theta}\right)-\rho_{nf}g(\cos\theta\cos\alpha) \quad (3)$$

where:
P_r - Prandtl number
μ_{nf} - Dynamic viscosity of the nanofluid (kg/m.s)
α - Angle of inclination cylinder (Degree)

θ – Component

$$\rho_{nf}\left(u\frac{\partial v}{\partial r}+\frac{v}{r}\frac{\partial v}{\partial\theta}+\frac{uv}{r}\right)=-\frac{1}{r}\frac{\partial p}{\partial\theta}+\mu_{nf}\left(\frac{\partial^2v}{\partial r^2}+\frac{1}{r}\frac{\partial v}{\partial r}+\frac{1}{r^2}\frac{\partial^2v}{\partial\theta^2}-\frac{v}{r^2}+\frac{2}{r^2}\frac{\partial v}{\partial\theta}\right)-\rho_{nf}g(\sin\theta\cos\alpha) \quad (4)$$

z - Component

$$\rho_{nf}\left(u\frac{\partial w}{\partial r}+\frac{v}{r}\frac{\partial w}{\partial\theta}\right)=-\frac{\partial p}{\partial z}+\mu_{nf}\left(\frac{\partial^2w}{\partial r^2}+\frac{1}{r}\frac{\partial w}{\partial r}+\frac{1}{r^2}\frac{\partial^2w}{\partial\theta^2}\right)-\rho_{nf}g(\sin\alpha) \quad (5)$$

$$\rho_{nf}=(1-\theta)\rho_f+\theta\rho_s \quad (6)$$

where:

$\boldsymbol{\rho_f}$ - Density of fluid (kg/m^3)

$\boldsymbol{\rho_s}$ - Density of solid (kg/m^3)

Inner wall temperature at each section is expressed by:

$$t_w=t_{wo}+\left(\frac{\partial t}{\partial z}\right)_w \quad (7)$$

Global Digital Central
ISSN: 2151-8629

The temperatures gradient in the axial direction is constant$\left(\frac{\partial t}{\partial z}\right)_w =$ B, and two represents the temperature of the wall at the starting section of the thermally fully developed region, where tw is the all temperature (°C).

Energy Equation

The energy equation in the cylindrical coordinates takes the following form, (Shareef et al., 2010).

$$\rho_{nf}c_{pnf}\left(u\frac{\partial t}{\partial r}+\frac{v}{r}\frac{\partial t}{\partial \theta}+w\frac{\partial t}{\partial z}\right)=k_{nf}\left(\frac{1}{r}\frac{\partial}{\partial r}\left(r\frac{\partial t}{\partial r}\right)+\frac{1}{r^2}\frac{\partial^2 t}{\partial \theta^2}+\frac{\partial^2 t}{\partial z^2}\right) \quad (8)$$

where:

c_{pnf} - Specific heat of nanofluid at constant pressure (kJ/kg.K)

k_{nf} - Thermal conductivity of the nanofluid (W/m.K)

Since $(\frac{\partial t}{\partial z})$ is constant along axis in the direction of the main flow (z– direction).Therefore, $\frac{\partial^2 t}{\partial z^2}=0$, and eq. (8) will be:

$$\left(u\frac{\partial t}{\partial r}+\frac{v}{r}\frac{\partial t}{\partial \theta}\right)=\alpha_{nf}\left(\frac{1}{r}\frac{\partial}{\partial r}\left(r\frac{\partial t}{\partial r}\right)+\frac{1}{r^2}\frac{\partial^2 t}{\partial \theta^2}\right)-w\frac{\partial t}{\partial z} \quad (9)$$

where:

α_{nf} : Thermal diffusivity of the nanofluid (m^2/s)

The physical properties of the nanofluid that are taken as function of the volume fraction are defined as follows:

Effective thermal conductivity

Effective thermal conductivity calculates by the following (Azeez et al., 2020).

$$k_{nf}=\left[\frac{k_s+(n-1)k_f-(n-1)\Phi(k_f-k_s)}{k_s+(n-1)k_f+\Phi(k_f-k_s)}\right]k_f \quad (10)$$

where:

n - Shape factor and equals to 3 for spherical nanoparticles

k_s - Thermal conductivity of the solid (W/m.K)

k_f - Thermal conductivity of the fluid (W/m.K)

Φ - Volume fraction (Vol. %)

Thermal diffusivity

Thermal diffusivity of nanofluids calculates from the following formula (Hussein et al., 2016).

$$\alpha_{nf}=\frac{k_{nf}}{(1-\Phi)(\rho c_p)_f+\Phi(\rho c_p)_s} \quad (11)$$

Thermal expansion coefficient

Thermal expansion of nanofluids evaluates by the following equation (Hussein et al., 2017).

$$\beta_{nf}=\left[\left(\frac{1}{1+\frac{(1-\Phi)\rho_f}{\Phi\rho_s}}\right)\left(\frac{\beta_f}{\beta_s}\right)+\left(\frac{1}{1+\frac{\Phi\rho_s}{(1-\Phi)\rho_f}}\right)\right] \quad (12)$$

where:

β_{nf} - Thermal expansion coefficient of the nanofluid (1/K)

β_f - Thermal expansion coefficient of the fluid (1/K)

β_s - Thermal expansion coefficient of the solid (1/K)

Specific heat

Following formula used to calculate specific heat of nanofluids (Hussein et al., 2017).

$$c_{pnf}=\left[\frac{(1-\Phi)(\rho c_p)_f+\Phi(\rho c_p)_s}{(1-\Phi)\rho_f+\Phi\rho_s}\right] \quad (13)$$

Effective viscosity

Following formula used to calculate effective viscosity of nanofluids (Abed et al., 2020).

$$\mu_{nf}=[123\Phi^2+7.3\Phi+1] \quad (14)$$

2. Transformation of the Governing Equations into Non – Dimensional Form

The pressure term can be eliminated from the equations of momentum in directions $(r,\theta)$by cross differentiating between two momentum components. Differentiation of eq. (3) with respect to θ and r gives:

$$u\frac{\partial^2 u}{\partial r\partial\theta}-\frac{u}{r}\frac{\partial u}{\partial\theta}+v\frac{\partial^2 v}{\partial r\partial\theta}-v\frac{\partial\Omega}{\partial\theta}-\frac{v}{r}\frac{\partial v}{\partial\theta}=-\frac{1}{\rho_{nf}}\frac{\partial^2 p}{\partial r\partial\theta}+\nu_{nf}\left(\frac{\partial}{\partial\theta}\left(\frac{\partial^2 u}{\partial r^2}\right)+\frac{1}{r}\frac{\partial^2 u}{\partial r\partial\theta}+\frac{1}{r^2}\frac{\partial^3 u}{\partial\theta^3}-\frac{1}{r^2}\frac{\partial u}{\partial\theta}-\frac{2}{r^2}\frac{\partial^2 v}{\partial\theta^2}-g\beta_{nf}\left(\Delta t\sin\theta+\cos\theta\frac{\partial t}{\partial\theta}\right)\cos\alpha\right) \quad (15)$$

where:
Ω – Vorticity (1/s)
ν_{nf} - Kinematic viscosity of nanofluids (m^2/s)
g – Gravity acceleration (m/s^2)
β_{nf} – Thermal expansion coefficient of the nanofluid (1/K)
p – Pressure (N/m2)
Δt – Difference between temperatures (°C)
t - Temperature (°C)

$$ru\frac{\partial\Omega}{\partial r}+u\frac{\partial^2 u}{\partial r\partial\theta}-\frac{u}{r}\frac{\partial u}{\partial\theta}+\frac{uv}{r}-rv\frac{\partial^2 u}{\partial r^2}-v\frac{\partial u}{\partial r}=-\frac{1}{\rho_{nf}}\frac{\partial^2 p}{\partial r\partial\theta}+\nu_{nf}\left(r\frac{\partial^3 v}{\partial r^3}+2\frac{\partial^2 v}{\partial r^2}+\frac{1}{r}\frac{\partial}{\partial r}\left(\frac{\partial^2 v}{\partial\theta^2}\right)-\frac{1}{r}\frac{\partial v}{\partial r}+\frac{v}{r}+\frac{2}{r}\frac{\partial^2 v}{\partial r\partial\theta}-\frac{2}{r^2}\frac{\partial u}{\partial\theta}\right)+g\beta_{nf}\sin\theta\left(r\frac{\partial t}{\partial r}+\Delta t\right)\cos\alpha \quad (16)$$

By subtracting eq. (15) from eq. (16), dividing by r and rearranging, the following equation can be obtained:

$$-\frac{v}{r}\frac{\partial\Omega}{\partial\theta}-u\frac{\partial\Omega}{\partial r}=\nu_{nf}\left(-\frac{\partial^2\Omega}{\partial r^2}-\frac{1}{r}\frac{\partial\Omega}{\partial r}-\frac{1}{r^2}\frac{\partial^2\Omega}{\partial\theta^2}\right)-g\beta_{nf}\left(\frac{\cos\theta}{r}\frac{\partial t}{\partial\theta}+\sin\theta\frac{\partial t}{\partial r}\right)\cos\alpha \quad (17)$$

The stream function in the cylindrical coordinates is defined as:

$u=\frac{1}{r}\frac{\partial\Psi}{\partial\theta}$, and $v=-\frac{\partial\Psi}{\partial r}$

As a result, eq. (17) can be reduced into following form:

$$\frac{1}{r}\left(\frac{\partial\Psi}{\partial\theta}\frac{\partial\Omega}{\partial r}-\frac{\partial\Psi}{\partial r}\frac{\partial\Omega}{\partial\theta}\right)=\nu_{nf}\left(\frac{\partial^2\Omega}{\partial r^2}+\frac{1}{r}\frac{\partial\Omega}{\partial r}+\frac{1}{r^2}\frac{\partial^2\Omega}{\partial\theta^2}\right)+g\beta_{nf}\left(\frac{\cos\theta}{r}\frac{\partial t}{\partial\theta}+\sin\theta\frac{\partial t}{\partial r}\right)\cos\alpha \quad (18)$$

The momentum equations in the (z,r,θ)directions and energy equation take respectively the following forms:

$$\rho_{nf}\left(\frac{\partial w}{\partial\tau}+\frac{1}{r}\frac{\partial\Psi}{\partial\theta}\frac{\partial w}{\partial r}-\frac{1}{r}\frac{\partial\Psi}{\partial r}\frac{\partial w}{\partial\theta}\right)=-\frac{\partial p}{\partial z}+\mu_{nf}\left(\frac{\partial^2 w}{\partial r^2}+\frac{1}{r}\frac{\partial w}{\partial r}+\frac{1}{r^2}\frac{\partial^2 w}{\partial\theta^2}\right)-\rho_{nf}g\sin\theta \quad (19)$$

where:
τ - Time (s)

Global Digital Central
ISSN: 2151-8629

$$\frac{\partial\Omega}{\partial\tau}+\frac{1}{r}\left(\frac{\partial\Psi}{\partial\theta}\frac{\partial\Omega}{\partial r}-\frac{\partial\Psi}{\partial r}\frac{\partial\Omega}{\partial\theta}\right)=\nu_{nf}\left(\frac{\partial^2\Omega}{\partial r^2}+\frac{1}{r}\frac{\partial\Omega}{\partial r}+\frac{1}{r^2}\frac{\partial^2\Omega}{\partial\theta^2}\right)+g\beta_{nf}\left(\frac{\cos\theta}{r}\frac{\partial t}{\partial\theta}+\sin\theta\frac{\partial t}{\partial r}\right)\cos\alpha\alpha \quad (20)$$

where:

ν_{nf} - Kinematics viscosity of nanofluids (m^2/s)

$$\frac{\partial t}{\partial\tau}+\frac{1}{r}\frac{\partial\Psi}{\partial\theta}\frac{\partial t}{\partial r}-\frac{1}{r}\frac{\partial\Psi}{\partial r}\frac{\partial t}{\partial\theta}=\alpha_{nf}\left[\frac{1}{r}\frac{\partial}{\partial r}\left(r\frac{\partial t}{\partial r}\right)+\frac{1}{r^2}\frac{\partial^2 t}{\partial\theta^2}\right]-w\frac{\partial t}{\partial z} \quad (21)$$

The equation of vorticity in the cylindrical coordinates can be written as:

$$\nabla^2\Psi=-\Omega \quad (22)$$

$$\Omega=\frac{\partial v}{\partial r}+\frac{v}{r}-\frac{1}{r}\frac{\partial v}{\partial\theta} \quad (23)$$

By substituting the following non – dimensional parameters:

$\lambda=\frac{\alpha}{R^2}\tau$, $W=\frac{w}{\overline{W}}$, $\Psi=\frac{\Psi}{\alpha_{nf}}$, $R=\frac{r}{R}$, $Z=\frac{z}{R}$, $P=\frac{pR}{\rho\overline{W}\alpha_{nf}}$, $T=\frac{t-t_b}{\frac{2\ddot{q}_w R}{k_{nf}}}$, $\xi=\frac{R^2\Omega}{\alpha_{nf}}$, $G=\frac{gR^2}{\alpha_{nf}\overline{W}}$

where:
λ – Dimensionless time
R – *Dimensionless* radius
Ψ - Dimensionless stream function
W – *Dimensionless* axial velocity in Z direction
$\overline{W}$ – Mean axial velocity (m/s)
P – Dimensionless pressures
T - Dimensionless temperature
t_b – Bulk temperature (^oC)
$\ddot{q}_w$ - Heat flux (W/m^2)
G - Dimensionless gravity acceleration

Mean axial velocity evaluate from the following equation (Holman, 2010).

$$\overline{W}=\frac{2}{\pi r_o^2}\int_0^{\pi}\int_0^{r_o}Wrdrd\theta \quad (24)$$

Bulk temperature evaluate from the following equation (Kaviany, 2012).

$$t_b=\frac{2}{\dot{m}_{nf}c_{pnf}}\int_0^{\pi}\int_0^{r_o}\rho_{nf}c_{pnf}Wtrdrdr\theta \quad (25)$$

Where:
$\dot{m}_{nf}$ - Mass flow rate of nanofluids (kg/s)

From equations (19) and (23) give:

$$\frac{\partial W}{\partial\lambda}+\frac{1}{R}\left(\frac{\partial\Psi}{\partial\theta}\frac{\partial W}{\partial R}-\frac{\partial\Psi}{\partial R}\frac{\partial W}{\partial\theta}\right)=-\frac{\partial p}{\partial z}+Pr_{nf}\nabla^2W-Gsin\alpha \quad (26)$$

where:
Pr_{nf} - Prandtl number for nanofluid

$$\frac{\partial\xi}{\partial\lambda}+\frac{1}{R}\left(\frac{\partial\Psi}{\partial\theta}\frac{\partial\xi}{\partial R}-\frac{\partial\Psi}{\partial R}\frac{\partial\xi}{\partial\theta}\right)=\frac{\nu_{nf}}{\alpha}\nabla^2\xi+\frac{g\beta\ddot{q}_w R^4}{k_{nf}\alpha_{nf}^2}\left(\frac{\cos\theta}{R}\frac{\partial T}{\partial\theta}+\sin\theta\frac{\partial T}{\partial R}\right)\cos\alpha \quad (27)$$

The final form of non – dimensional and momentum equations in (r,θ) and z directions will be:

$$\frac{\partial\xi}{\partial\lambda}+\frac{1}{R}\left(\frac{\partial\Psi}{\partial\theta}\frac{\partial\xi}{\partial R}-\frac{\partial\Psi}{\partial R}\frac{\partial\xi}{\partial\theta}\right)=Pr_{nf}\nabla^2\xi+Pr_{nf}Ra_{nf}\left(\frac{\cos\theta}{R}\frac{\partial T}{\partial\theta}+\sin\theta\frac{\partial T}{\partial R}\right)\cos\alpha \quad (28)$$

where:
Ra_{nf} - Rayleigh number of nanofluid

Since the pressure gradient along the pipe axis is constant, then the axial density gradient can be neglected.

$$W=\widehat{W}\frac{\partial p}{\partial z} \quad (29)$$

Where:
$\widehat{W}$ - Dimensionless velocity in z direction
By dividing eq. (26) by $\frac{\partial p}{\partial z}$ and substituting eq. (29) in itself, the following equation can be obtained:

$$\frac{\partial\widehat{W}}{\partial\lambda}=-\frac{1}{R}\left(\frac{\partial\Psi}{\partial\theta}\frac{\partial\widehat{W}}{\partial R}-\frac{\partial\Psi}{\partial R}\frac{\partial\widehat{W}}{\partial\theta}\right)-1+Pr_{nf}\nabla^2\widehat{W}-\frac{G}{\frac{\partial p}{\partial z}}\sin\alpha \quad (30)$$

Since the average velocity remains constant, the pressure gradient $\frac{\partial p}{\partial z}$ takes the following integral form:

$$\frac{\partial p}{\partial z}=\frac{\pi}{\int_0^{\pi}\int_0^1\widehat{W}RdRd\theta} \quad (31)$$

Applying Simpson's rule to the double integral which includes the definition of a new function, (F) taking the following form:

$$F=\widehat{W}(R,\theta).R \quad (32)$$

The velocity at each node will be multiplied by the radius of this node, and eq. (29) becomes as follows:

$$\frac{\partial p}{\partial z}=\frac{\pi}{\int_0^{\pi}\int_0^1 F(R,\theta)dRd\theta} \quad (33)$$

The equation of energy, eq. (21) can be simplified as follows:

$$\frac{\partial t}{\partial\tau}+\frac{1}{r}\left(\frac{\partial\Psi}{\partial\theta}\frac{\partial t}{\partial r}-\frac{\partial\Psi}{\partial r}\frac{\partial t}{\partial\theta}\right)=\alpha_{nf}\nabla^2t-W\frac{\partial t}{\partial z} \quad (34)$$

Substituting the non – dimensional parameters in the energy equation gives:

$$\frac{\partial T}{\partial\lambda}+\frac{1}{R}\left(\frac{\partial\Psi}{\partial\theta}\frac{\partial T}{\partial R}-\frac{\partial\Psi}{\partial R}\frac{\partial T}{\partial\theta}\right)=\nabla^2T-W\widehat{W}\frac{R}{\alpha_{nf}}\frac{\partial T}{\partial z} \quad (35)$$

But (Holman, 2010).

$$\frac{\partial T}{\partial z}=\frac{2\alpha_{nf}}{R\widehat{W}} \quad (36)$$

Then:

$$\frac{\partial T}{\partial\lambda}+\frac{1}{R}\left(\frac{\partial\Psi}{\partial\theta}\frac{\partial T}{\partial R}-\frac{\partial\Psi}{\partial R}\frac{\partial T}{\partial\theta}\right)=\nabla^2T-2W \quad (37)$$

The equation of vorticity in terms of stream function is an elliptic partial differential equation and can be represented in the following non – dimensional form (Kaviany, 2012).

$$\nabla^2\Psi=-\xi \quad (38)$$

Where:

$$\nabla^2\Psi=\frac{\partial^2\Psi}{\partial R^2}+\frac{1}{R}\frac{\partial\Psi}{\partial R}+\frac{1}{R^2}\frac{\partial^2\Psi}{\partial\theta^2} \quad (39)$$

3. Boundary Conditions

Table 1 represents of the boundary conditions of this study.

Surface	*Stream line* Ψ	*Axial velocity* $\widehat{W}$	*Temperature* T	*Vorticity* ξ
Symmetry wall	$\Psi(R,0,Z_F)=0$ $\Psi(R,\pi,Z_F)=0$	$\widehat{W}_\theta(R,0,Z_F)=0$ $\widehat{W}_\theta(R,\pi,Z_F)=0$	$T_\theta(R,0,Z_F)=0$ $T_\theta(R,\pi,Z_F)=0$	$\xi(R,0,Z_z)=0$ $\xi(R,0,Z_F)=0$

Global Digital Central
ISSN: 2151-8629

External surface wall	$\Psi(1,\theta,Z_F)=0$ $\Psi(1,0,Z_F)=0$ $\Psi(1,\pi,Z_F)=0$ $\Psi_R(1,\theta,Z_F)=0$ $\Psi_{\theta R}(1,\theta,Z_F)=0$	$\widehat{W}(1,\theta,Z_F)=0$	$T(1,\theta,Z_F)=\frac{1}{2Nu}$	

4. Grid Testing and Validation

Basically, the flow region associated with the polar coordinates (R, θ) is divided into a grid network which contains the following dimensions (ΔR*Δθ) for one division as shown in Fig. 2.

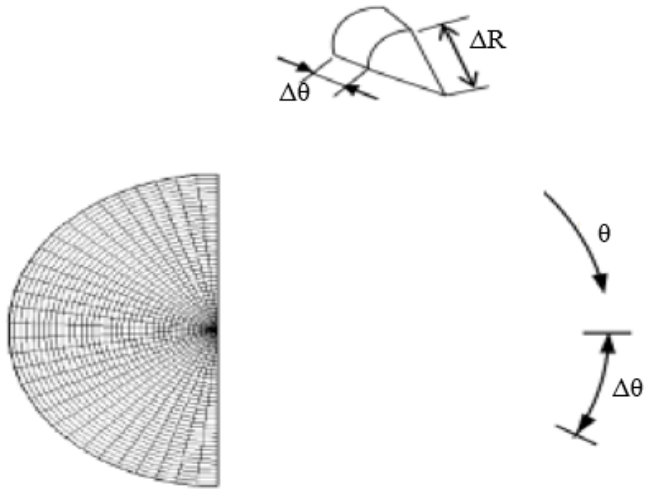

Fig. 2 Mesh network for flow region representation

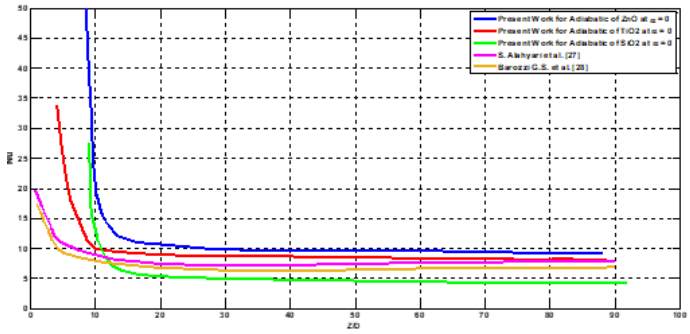

Fig. 3 Comparison of the axial evolution of Nu in a horizontal tube with the corresponding numerical results of S. Alahyari et al. And with experimental results of Barozzi et al.

After doing grid independence tests to demonstrate the validity and also precision of the model and the numerical procedure, comparisons with the previously published experimental and numerical simulation have performance. Fig. 3 shows the comparison of the calculated results with the numerical results of S. Alahyari et al. (2010) in a horizontal tube. Another comparison has also been performed with the experimental results obtained by Barozzi et al. (1985) in a horizontal tube. It should be mentioned that our numerical results were obtained using the nanoparticles ZnO (30 nm), TiO2 (30 nm) and SiO2 (30 nm) with Ethylene – Glycol (EG) and volume fraction percentage (vol. = 2%) for adiabatic process. Therefore the numerical procedure is reliable and can predict developing mixed convection flow in a horizontal tube.

5. Numerical implementation

The governing equation in the cylindrical coordinates (equations 1, 2, 3,4and 5) as well as boundary conditions were discretized by finite difference method. In this study the finite difference equation were derived by using central difference approximation for the partial derivatives except the convective terms for which upwind difference formula was employed. Derivative at the boundary were approximated by three point forward backward difference. The explicit method was chose for the solution of flow and energy fields, while relaxation method was chose for stream function calculation. A time increment Δt =10-5 has been used for Ra=106. In order to evaluate how the presence of the Nanofluids affect the heat transfer rate around the perimeter of pipe according to the parameters Rayleigh number, Nano particles volume fraction, and theta it is necessary to observe the variation of the Local Nusselt number on the perimeter of pipe. In generalized coordinate the local and average Nusslet number defined as:

The local Nusselt number around the perimeter of tube will be as follows:

$$Nu_{nt}^{k+1} = \frac{Nu^k}{\Delta R}\left[3T_{mt,n}^k - 4T_{mt-1,n}^k + T_{mt-2,n}^k\right] \quad (40)$$

The mean Nusselt number around the perimeter of pipe at location (k+1) is deduced by integrating local Nusselt number as follows:

$$Nu^{k+1} = SNu^k + (1-S)\frac{2}{\pi}\int_0^{\pi} Nu_{nt}^{k+1} d\emptyset \quad (41)$$

The Nusselt number is used to calculate the surface temperature at the location (k+1), but it is found that the boundary conditions causes unstable state in the solution at the value of relaxation factor (S=0). Therefore; relaxation factor (S=0.8) is used for stability considerations (Thomas et al., 2003). The above integral was calculated using Simpson's rule 1/3 method. To show the effect of the nanofluids on heat transfer rate, we introduce a variable called Nusselt number ratio (NUR) with its definition given as:

$$NUR = \frac{Nu_{ave}|\text{with nanofluid}}{Nu_{ave}|\text{ pure fluid}}$$

If the value of NUR greater than 1 indicated that the heat transfer rate is enhanced on that fluid, whereas reduction of heat transfer is indicated when NUR is less than 1 (Fadhil et al. , 2019).

6. Thermo physical Properties

Table 2 Thermo physical properties of base liquid types.

Base Liquid Type	Density (kg/m^3)	Specific Heat (J/kg.K)	Viscosity (kg/m.s)	Thermal Conductivity (W/m.K)	Pr
Water	997	4170	$1.00*10^{-3}$	0.606	6.96
Ethylene – Glycol (EG)	1111	2415	$1.57*10^{-2}$	0.252	150.46

Global Digital Central
ISSN: 2151-8629

The present study was conducted for both the constant heat flux (q''_w = 10,000 W/m^2) and constant wall temperature (T_w = 313.15 K) boundary conditions. At the inlet, the uniform axial velocity u_o and initial temperature (T_o = 293 K) were assumed. The thermo physical properties of the base fluids (60% ethylene glycol and 40% water) and nanoparticles (TiO_2 (30 nm), SiO_2 (30 nm), ZnO (30 nm)) are specified in tables 2 and 3, respectively. These properties were adopted from Al-damook et al. (2020), Al-damook et al. (2020) and Abed and Afgan (2020).

Table 3 Thermo physical properties of different nanoparticles types.

Nanoparticles Type	Density (kg/m^3)	Specific Heat (J/kg.K)	Thermal Conductivity (W/m.K)
TiO_2	3900	692	8.40
SiO_2	2200	745	1.40
ZnO	5600	495	13

7. Results and Discussion:

Fig. 4 represents the relation between the variations of Nusselt number (Nu) with angle of inclination cylinder (α) for adiabatic process of ZnO nanoparticles at Reynolds number (Re = 400), Rayleigh number (Ra = 10^6) and volume fraction percentage (vol. = 2%). In general, increasing the slop up to α=45^0, the Nusselt number augments, while Nusselt number is reduced by further tube inclination. As it is clearly seen, the highest value of Nusselt number is corresponded to α=45^0.

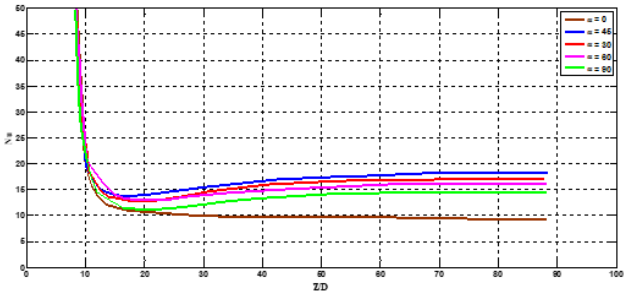

Fig. 4 Variation of Nu with α for adiabatic of ZnO at Re = 400, Ra = 10^6 and Φ = 2 vol. %.

Fig. 5 shows the relation between the variations of Nusselt number (Nu) with angle of inclination cylinder (α) for adiabatic process of TiO_2 nanoparticles at Reynolds number (Re = 400), Rayleigh number (Ra = 10^6) and volume fraction percentage (vol. = 2%). In general, increasing the slop up to α=45^0, the Nusselt number augments, while Nusselt number is reduced by further tube inclination. As it is clearly seen, the highest value of Nusselt number is corresponded to α=45^0.

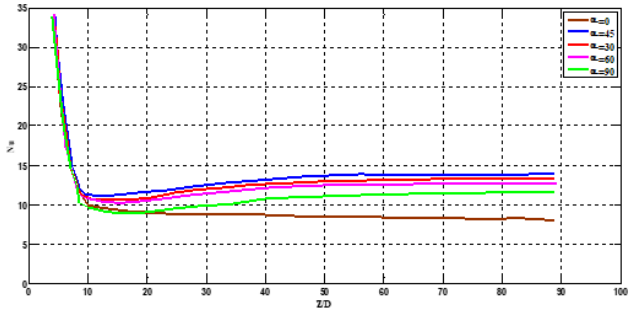

Fig. 5 Variation of Nu with α for adiabatic of TiO_2 at Re = 400, Ra = 10^6 and Φ = 2 vol. %.

Fig. 6 represents the relation between the variations of Nusselt number (Nu) with angle of inclination cylinder (α) for adiabatic process of SiO_2 nanoparticles at Reynolds number (Re = 400), Rayleigh number (Ra = 10^6) and volume fraction percentage (vol. = 2%). In general, increasing the slop up to α=45^0, the Nusselt number augments, while Nusselt number is reduced by further tube inclination. As it is clearly seen, the highest value of Nusselt number is corresponded to α=45^0.

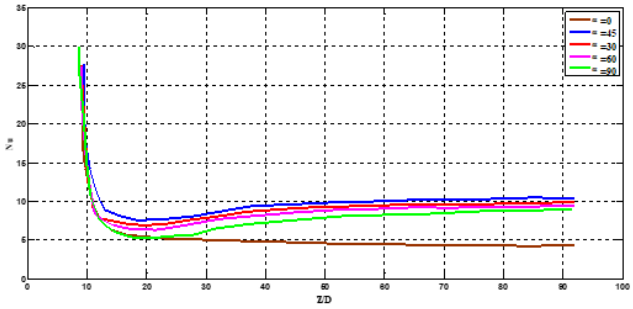

Fig. 6 Variation of Nu with α for adiabatic of SiO_2 at Re = 400, Ra = 10^6 and Φ = 2 vol. %.

Fig. 7 represents the relation between the variations of Nusselt number (Nu) with angle of inclination cylinder (α) for isothermal process of ZnO nanoparticles at Reynolds number (Re = 400), Rayleigh number (Ra = 10^6) and volume fraction percentage (vol. = 2%). It is clearly shown that increasing the Nusselt number in horizontal position of the isothermal case is higher than the vertical position.

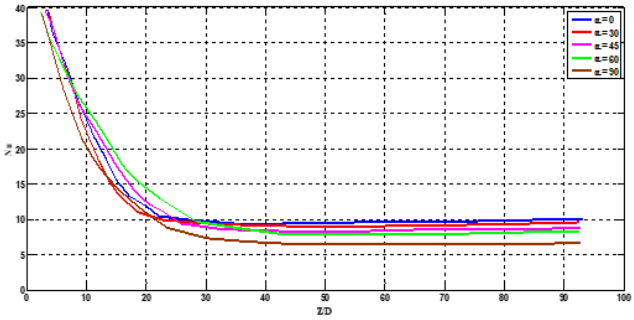

Fig. 7 Variation of Nu with α for isothermal of ZnO at Re = 400, Ra = 10^6 and Φ = 2 vol. %.

Fig. 8 shows the relation between the variations of Nusselt number (Nu) with angle of inclination cylinder (α) for isothermal process of TiO_2 nanoparticles at Reynolds number (Re = 400), Rayleigh number (Ra = 10^6) and volume fraction percentage (vol. = 2%). It is clearly shown that increasing the Nusselt number in horizontal position of the isothermal case is higher than the vertical position.

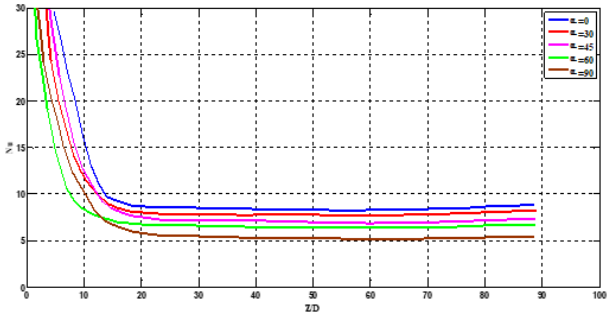

Fig. 8 Variation of Nu with α for isothermal of TiO_2 at Re = 400, Ra = 10^6 and Φ = 2 vol. %.

Fig. 9 represents the relation between the variations of Nusselt number (Nu) with angle of inclination cylinder (α) for isothermal process of SiO_2 nanoparticles at Reynolds number (Re = 400), Rayleigh number (Ra = 10^6) and volume fraction percentage (vol. = 2%). It is clearly shown that increasing the Nusselt number in horizontal position of the isothermal case is higher than the vertical position.

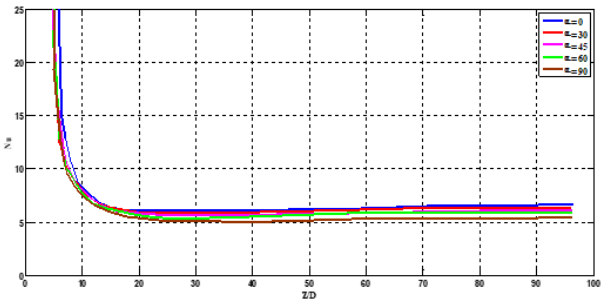

Fig. 9 Variation of Nu with α for isothermal of SiO_2 at Re = 400, Ra = 10^6 and Φ = 2 vol. %.

8. Conclusions

The present study was carried out to investigate about effect nanofluids flow of nanoparticles of ZnO, TiO_2 and SiO_2 base fluids (60% ethylene glycol and 40% water) (through horizontal and inclined cylinder on the Nusselt number for adiabatic and isothermal process, the flow at Reynolds number (Re = 400), Rayleigh number (Ra = 10^6) and volume fraction percentage (vol. = 2%), from results we can conclude the following:

1. For adiabatic process when increasing the slop up to α=45^0, the Nusselt number augments, while Nusselt number is reduced by further tube inclination. As it is clearly seen, the highest value of Nusselt number is corresponded to α=45^0. Nusselt number of ZnO is greater than of TiO_2 and SiO_2, because thermal conductivity of ZnO is higher than of TiO_2 and SiO_2.
2. For isothermal process Nusselt number in horizontal position of the isothermal case is higher than at the vertical position. For this process Nusselt number of ZnO is greater than of TiO_2 and SiO_2, because thermal conductivity of ZnO is higher than of TiO_2 and SiO_2.

NOMENCLATURE

c_{pnf}	specific heat of nanofluid at constant pressure (kJ/kg.K)
g	gravity acceleration (m/s^2)
k_{nf}	thermal conductivity of the nanofluid (W/m.K)
$\dot{m}$	Mass flow rate (kg/s)
Nu	Nusselt number
p	pressure (N/m^2)
P	dimensionless pressures
Pr_{nf}	Prandtl number of nano fluid
$\ddot{q}_w$	Heat flux (W/m^2)
R	dimensionless radius
Ra_{nf}	Rayleigh number of nanofluid
$(R, \emptyset)$	Radial and tangential direction
$(R, \emptyset, Z)$	Dimensionless cylindrical coordinates
r	tube radius (m)
S	relaxation factor
T	dimensionless temperature
t	temperature (°C)
t_w	wall temperature (°C)
t_b	Bulk temperature (°C)
u	radial velocity component (r) (m/s)
v	tangential velocity component (∅) (m/s)
W	dimensionless axial velocity in Z direction
w	axial velocity component (z) (m/s)
$\widehat{W}$	Dimensionless velocity in the Z direction
$\overline{W}$	Mean axial velocity (m/s)
Z	dimensionless axial coordinate
z	axial coordinate (m)

Greek Symbols

α	angle of inclination of the tube (degree)
α_{nf}	Thermal diffusivity of the nanofluid (m^2/s)
β_{nf}	The thermal expansion coefficient of the nanofluid (1/K)
λ	dimensionless time
μ_{nf}	dynamic viscosity of the nanofluid (kg/m.s)
ν_{nf}	kinematic viscosity of the nanofluid (m^2/s)
ξ	Dimensionless vorticity
ρ_{nf}	Density of the nanofluid (kg/m^3)
τ	Time (s)
Φ	volume fraction (Vol %)
ψ	Stream function (m2/s)
Ψ	Dimensionless stream function
Ω	vorticity (1/s)
∅	Tangential coordinate

Subscripts

b	bulk
bf	base fluid
f	fluid
m	mean
mt	number of radial points in the numerical mesh network
nt	number of tangential points in the numerical mesh network
s	solid
w	wall

Superscripts

k	time step
k+1	forward time step

REFERENCES

Abdellateef, A.I., 2016 Peristaltic Flow of Newtonian Nanofluid through Inclined Annulus Cylinder. *European Journal of Pure and Applied Mathematics*, *9*(3), pp. 266-276.

https://ejpam.com/index.php/ejpam/article/view/2502

Abed, N. and Afgan, I., 2020. An extensive review of various technologies for enhancing the thermal and optical performances of parabolic trough collectors. *International Journal of Energy Research*, *44*(7), pp.5117-5164.

https://doi.org/10.1002/er.5271

Abed, N., Afgan, I., Nasser, A., Iacovides, H., Cioncolini, A. and Mekhail, T., 2020. Numerical Investigations of parabolic trough collectors using different nanofluids. *International Journal of Applied Energy Systems*, *2*(2), pp.88-94.

https://dx.doi.org/10.21608/ijaes.2020.169898

Ahmed, S.E., Hussein, A.K., Mohammed, H.A. and Sivasankaran, S., 2014. Boundary layer flow and heat transfer due to permeable stretching tube in the presence of heat source/sink utilizing nanofluids. *Applied Mathematics and Computation*, *238*, pp.149-162.

https://doi.org/10.1016/j.amc.2014.03.106

Allahyari, S., Behzadmehr, A. and Sarvari, S.H., 2011. Conjugate heat transfer of laminar mixed convection of a nanofluid through a horizontal tube with circumferentially non-uniform heating. *International Journal of Thermal Sciences*, *50*(10), pp.1963-1972.

https://doi.org/10.1016/j.ijthermalsci.2011.03.025

Al-damook, A., Alfellag, M.A. and Khalil, W.H., 2020. Three-dimensional computational comparison of mini pinned heat sinks using different nanofluids: Part one—the hydraulic-thermal characteristics. *Heat Transfer—Asian Research*, *49*(1), pp.591-613.

https://doi.org/10.1002/htj.21628

Al-damook, A., Alfellag, M.A. and Khalil, W.H., 2020. Three-dimensional computational comparison of mini-pinned heat sinks using different nanofluids: Part two—energy and exergy characteristics. *Heat Transfer—Asian Research*, *49*(1), pp.441-460.

https://doi.org/10.1002/htj.21620

Azeez, K., Ibrahim, Z.A. and Hussein, A.M., 2020. Thermal conductivity and viscosity measurement of ZnO nanoparticles dispersing in various base fluids. *Journal of Advanced Research in Fluid Mechanics and Thermal Sciences*, *66*(2), pp.1-10.

https://www.akademiabaru.com/submit/index.php/arfmts/article/view/2818

Barozzi, G.S., Zanchini, E. and Mariotti, M., 1985. Experimental investigation of combined forced and free convection in horizontal and inclined tubes. *Meccanica*, *20*(1), pp.18-27.

https://doi.org/10.1007/BF02337057

Davarnejad, R. and Hekmat, M., 2018. Numerical study on influence of a type of nanoparticles and volume fraction on turbulent heat transfer coefficient and pressure loss inside a tube. *AUT Journal of Modeling and Simulation*, *50*(2), pp.123-128.

https://doi.org/10.22060/miscj.2018.13315.5069

Fadhil, A.M., Khalil, W.H. and Al-damook, A., 2019. The hydraulic-thermal performance of miniature compact heat sinks using SiO2-water nanofluids. *Heat Transfer—Asian Research*, *48*(7), pp.3101-3114.

https://doi.org/10.1002/htj.21532

Farhan, A.A., Obaid, Z.A.H. and Hussien, S.Q., 2020. Analysis of exergetic performance for a solar air heater with metal foam fins. *Heat Transfer*, *49*(5), pp.3190-3204.

https://doi.org/10.1002/htj.21769

Hekmatipour, F. and Jalali, M., 2020. Heat transfer and presser drop of copper oxide–thermal oil in upward single-phase flow in inclined microfin tube under constant wall temperature. *Journal of Thermal Analysis and Calorimetry*, *139*(3), pp.2203-2214.

https://doi.org/10.1007/s10973-019-08585-y

Hekmatipour, F., Akhavan-Behabadi, M.A., Sajadi, B. and Fakoor-Pakdaman, M., 2017. Mixed convection heat transfer and pressure drop characteristics of the copper oxide-heat transfer oil (CuO-HTO) nanofluid in vertical tube. *Case studies in thermal engineering*, *10*, pp.532-540.

https://doi.org/10.1016/j.csite.2017.09.009

Hekmatipour, F., Jalali, M. And Hekmatipour, F., 2019. Forced Convection and Pressure Drop Of CuO-TiO Nano-particle-fluid Inside Minus Slope Microfin Pipe Under Constant Wall Temperature. International Journal of Mechanical and Production Engineering Research and Development (IJMPERD), 9, pp.157-170.

http://dx.doi.org/10.24247/ijmperdoct201915

Heris, S.Z., Etemad, S.G. and Esfahany, M.N., 2006. Experimental investigation of oxide nanofluids laminar flow convective heat transfer. *International communications in heat and mass transfer*, *33*(4), pp.529-535.

https://doi.org/10.1016/j.icheatmasstransfer.2006.01.005

Holman, J.P., 2010. Unsteady Heat Conduction (Chapter 4). *Text Book "Heat Transfer, 10th Edition", McGrawHill Higher Education*.

http://dx.doi.org/10.13140/RG.2.2.12284.36488

Hussein, A.M., Bakar, R.A., Kadirgama, K. and Sharma, K.V., 2016. Heat transfer enhancement with elliptical tube under turbulent flow TiO2-water nanofluid. *Thermal Science*, *20*(1), pp.89-97.

http://dx.doi.org/10.2298/TSCI130204003H

Hussein, A.M., Dawood, H.K., Bakara, R.A. and Kadirgamaa, K., 2017. Numerical study on turbulent forced convective heat transfer using nanofluids TiO2 in an automotive cooling system. *Case Studies in Thermal Engineering*, *9*, pp.72-78.

https://doi.org/10.1016/j.csite.2016.11.005

Jalali, M., Hekmatipour, F. and Marofi, A., 2020. Experiment on the Forced Convection and Friction Factor of Nanofluid in Downward Flow in Slope Pipes. Journal of Mechanical Engineering Research and Developments 43(1), pp.18-35.

https://jmerd.net/01-2020-18-35/

Kandwal, S., Mishra, A. and Kumar, M., 2019. Numerical Investigation of Nanofluid Heat Transfer in an Inclined Stretching Cylinder under the Influence of Suction/Injection and Viscous Dissipation. *Nanoscience and Technology: An International Journal*, *10*(1).

http://dx.doi.org/10.1615/NanoSciTechnolIntJ.2018026365

Kaviany, M., 2012. *Principles of heat transfer in porous media*. Springer Science & Business Media.

https://link.springer.com/book/10.1007/978-1-4612-4254-3

Nguyen, C.T. and Le Menn, M., 2009. Two-phase modelling of nanofluid heat transfer in a microchannel heat sink. *vol*, *1*, pp.451-460.

https://doi.org/10.2495/CMEM09041

Qiu, L., Zhu, N., Feng, Y., Michaelides, E.E., Żyła, G., Jing, D., Zhang, X., Norris, P.M., Markides, C.N. and Mahian, O., 2020. A review of recent advances in thermophysical properties at the nanoscale: from solid state to colloids. *Physics Reports*, *843*, pp.1-81.

https://doi.org/10.1016/j.physrep.2019.12.001

Raei, B. and Peyghambarzadeh, S.M., 2019. Measurement of Local Convective Heat Transfer Coefficient of Alumina-Water Nanofluids in a Double Tube Heat Exchanger. *Journal of Chemical and Petroleum engineering*, *53*(1), pp.25-36.

https://dx.doi.org/10.22059/jchpe.2019.265521.1247

Sahoo, B.C., Das, D.K., Vajjha, R.S. and Satti, J.R., 2012. Measurement of the thermal conductivity of silicon dioxide nanofluid and development of correlations. *Journal of Nanotechnology in Engineering and Medicine*, *3*(4).

http://dx.doi.org/10.1115/1.4024003

Shareef, A.J., Abed, W.M. and Najeeb, A.A., 2010. Natural convection heat transfer in horizontal concentric annulus between outer cylinder and inner flat tube. *AJES*, *3*(2), p.31.

https://www.iasj.net/iasj/article/14222

Shariat, M., Akbarinia, A., Nezhad, A.H., Behzadmehr, A. and Laur, R., 2011. Numerical study of two phase laminar mixed convection nanofluid in elliptic ducts. *Applied Thermal Engineering*, *31*(14-15), pp.2348-2359.

https://doi.org/10.1016/j.applthermaleng.2011.03.035

Thomas, G.B., Finney, R.L., Weir, M.D. and Giordano, F.R., 2003. *Thomas' calculus*. Reading: Addison-Wesley.

https://lib.hpu.edu.vn/handle/123456789/33530